Signatures of Magnetic Separatrices at the Borders of a Crater Flux Transfer Event Connected to an Active X-Line

L. Trenchi[1,2] , J. C. Coxon[1] , R. C. Fear[1] , J. P. Eastwood[3] , M. W. Dunlop[4,5] , K. J. Trattner[6] , D. J. Gershman[7,8] , D. B. Graham[9] , Yu. Khotyaintsev[9] , and B. Lavraud[10]

[1]Department of Physics and Astronomy, University of Southampton, Southampton, UK, [2]Now at ESA-ESRIN, Directorate of Earth Observation Programmes, Rome, Italy, [3]The Blackett Laboratory, Imperial College London, London, UK, [4]School of Space and Environment, Beihang University, Beijing, China, [5]RAL_Space, STFC, Chilton, UK, [6]LASP, University of Colorado, Boulder, CO, USA, [7]NASA Goddard Space Flight Center, Greenbelt, MD, USA, [8]Department of Physics and the Institute for Physical Science and Technology, University of Maryland, College Park, MD, USA, [9]Swedish Institute of Space Physics, Uppsala, Sweden, [10]Institut de Recherche en Astrophysique et Planétologie, Université de Toulouse, CNRS, UPS, CNES, Toulouse, France

Abstract In this paper, we present Magnetospheric Multiscale (MMS) observations of a flux transfer event (FTE) characterized by a clear signature in the magnetic field magnitude, which shows maximum at the center flanked by two depressions, detected during a period of stable southward interplanetary magnetic field. This class of FTEs are called "crater-FTEs" and have been suggested to be connected with active reconnection X line. The MMS burst mode data allow the identification of intense fluctuations in the components of the electric field and electron velocity parallel to the magnetic field at the borders of the FTE, which are interpreted as signatures of the magnetic separatrices. In particular, the strong and persistent fluctuations of the parallel electron velocity at the borders of this crater-FTE reported for the first time in this paper, sustain the field-aligned current part of the Hall current system along the separatrix layer, and confirm that this FTE is connected with an active reconnection X line. Our observations suggest a stratification of particles inside the reconnection layer, where electrons are flowing toward the X line along the separatrix, are flowing away from the X line along the reconnected field lines adjacent to the separatrices, and more internally ions and electrons are flowing away from the X line with comparable velocities, forming the reconnection jets. This stratification of the reconnection layer forming the FTE, together with the reconnection jet at the trailing edge of the FTE, suggests clearly that this FTE is formed by the single X line generation mechanism.

1. Introduction

Magnetic reconnection at the dayside magnetopause is the main process that allows the entry of solar wind plasma and energy into the Earth's magnetosphere. This process, originally proposed by Dungey (1961), has been the subject of many studies based on in situ measurements of scientific spacecraft [see Paschmann et al., 2013 for a review]. While some effects of magnetic reconnection are visible in a large portion of the dayside magnetopause, like the bipolar perturbations of the magnetic field component normal to the magnetopause (Bn) associated with flux transfer events (FTEs; Lee & Fu, 1985; Russell & Elphic, 1978; Scholer, 1988; Southwood et al., 1988) or the accelerated plasma flows called reconnection jets (Paschmann et al., 1979), reconnection actually takes place inside a small diffusion region, located along the intersection of the magnetic separatrices called the X line, where the magnetic flux is no longer frozen into the motion of the ions and electrons (Burch et al., 2016).

In recent years it has been demonstrated that the diffusion region is constituted by two different parts. In the outer part, called the ion diffusion region, only the ions are decoupled from magnetic field lines, while the electrons remain frozen with the magnetic flux. Here the separation of ions and electrons generates a current system, called "Hall current system," that outside the diffusion region is closed by field aligned currents generated by electrons flowing toward the X line along the separatrices (Øieroset et al., 2001). According to the simulations of Wang et al. (2010) and Zenitani and Nagai (2016), these electrons flow toward the X line along the separatrices, would be reflected and accelerated at the X line, and would flow away from the X line

along the reconnected field lines adjacent to the separatrices. Geotail observations in the near-Earth magnetotail suggested that the Hall current system near the separatrix layer is formed by a thin double-sheet structure, consisting mostly of field aligned currents (Nagai et al., 2003).

The Hall current system, in turn, induces a quadrupolar perturbation of the out-of-plane magnetic field component (guide field; Øieroset et al., 2001; Eastwood et al., 2010). Given his small size, the ion diffusion region is generally identified with magnetic field data, which have usually much higher time resolution than plasma data, through the quadrupolar signature in the out-of-plane magnetic field component (Mozer et al., 2002; Nagai et al., 2001; Øieroset et al., 2001; Vaivads et al., 2004). Mistry et al. (2016) showed that Hall magnetic fields can also be observed far outside the ion diffusion region. Retinò et al. (2006) reported the presence of strong electric field fluctuations, electron beams and intense wave turbulence along the separatrices in proximity to the diffusion region, while other studies also highlighted the presence of low energy electron beams in proximity of the diffusion region flowing toward the X line along the separatrices (Fujimoto et al., 1997; Nagai et al., 2001; Øieroset et al., 2001) and also away from the X line (Hwang et al., 2017; Wang et al., 2010).

In the inner part of the diffusion region, called the electron diffusion region, the electrons are also decoupled from magnetic field lines. The processes inside the electron diffusion region are known mostly from numerical simulations. The first observations in proximity to the X line were performed by Geotail in the magnetotail reconnection (Nagai et al., 2011), and (Zenitani et al., 2012) estimated the energy dissipation in the rest frame of the electron's bulk flow. More recently the high time resolution observations of NASA Magnetospheric Multiscale (MMS) mission has provided detailed measurements within the electron diffusion region of magnetic reconnection at the dayside magnetopause (Burch et al., 2016; Hwang et al., 2017; Wang, Nakamura, et al., 2017)

Reconnection jets, which are jets of plasma accelerated away from the X line (northward and southward) by the magnetic tension of reconnected field lines, can be detected also when the spacecraft is located several Earth radii away from the X line. For this reason, if only unidirectional reconnection jets are sampled, this indicates that reconnection is active somewhere at the magnetopause, northward or southward of the spacecraft according to the direction of the reconnection jets, and that the spacecraft remains on the same side of the X line. On the other hand, if both the northward and the southward reconnection jets are sampled in a short time interval (jet reversal events), this indicates that the spacecraft is near the X line. Indeed, these jet reversal events can provide information about the position of the X line, and they have played an important role both to define statistically the global configuration of reconnection at the magnetopause, defining the location and the extension of the X line for the different interplanetary magnetic field (IMF) orientations (Trattner et al., 2012; Trenchi et al., 2008, 2009; Trenchi et al., 2015), but also to identify the intervals when the spacecraft is inside the diffusion region and to study the physical processes responsible for magnetic reconnection inside the diffusion region (Burch et al., 2016; Eastwood et al., 2010; Øieroset et al., 2001; Phan et al., 2016; Wang, Nakamura, et al., 2017).

Bipolar perturbations of B_N, first identified by Russell and Elphic (1978), are caused by the passage of magnetic field structures generated by time varying reconnection, which propagate along the magnetopause, and are referred to as FTEs. According to the different models, the FTEs can be formed by a reconnection burst along a short X line (Russell & Elphic, 1978), a burst of the reconnection rate along an extended X line (Scholer, 1988; Southwood et al., 1988), or time varying reconnection along multiple extended X lines (Lee & Fu, 1985). (See Fear et al., 2008 for further discussion of the differences between these mechanisms). The polarity of the B_N signature gives information about the relative position of the spacecraft with respect to the X line: a positive-negative (standard polarity) signature is observed when the spacecraft is northward of the X line, while a negative-positive (reverse polarity) signature is seen when the spacecraft is southward of the X line (Rijnbeek et al., 1984). There has been some disconnect in estimates of the amount of flux transferred by FTEs as calculated from ground-based data and in situ data, but these estimates can be reconciled to show that FTEs are likely to be the largest method of flux transfer from the solar wind to the magnetosphere (Fear et al., 2017).

MMS is the ideal mission to study FTEs, given the higher time resolution with respect to previous missions, the excellent intercalibration of plasma and field instruments among the four spacecraft, and the close formation, with a minimum separation among the spacecraft of about 10 km in Phase 1a (Burch et al., 2015). This allows MMS to determine the currents with unprecedented time resolution, with the curlometer

technique (Dunlop et al., 2002; Robert et al., 1998) at smaller scales with respect to the previous missions, or directly from the ion and electron velocities measured by the plasma instrument (Phan et al., 2016). The precise determination of the currents inside the FTEs allows investigation of the force balance, assessing the validity of the force-free assumption inside the FTEs.

Zhao et al. (2016) analyzed four FTEs with MMS data estimating the currents with the curlometer technique, and found that in some cases the force free assumption is satisfied, that is, the current is essentially field aligned and the magnetic pressure force is balanced by the magnetic tension force; however, in other FTEs the perpendicular component of the current is not negligible, and also the ion pressure plays a role in the force balance. Farrugia et al. (2016) estimated the current directly from ion and electron velocities measured by the plasma instrument onboard MMS, and analyzed a single FTE that does not satisfy the force free approximation, modeling the FTE with a non-force free circular flux rope model. Eastwood et al. (2016) studied two ion-scale FTEs, and computed the currents using both the curlometer and the plasma data, finding a very good agreement between the two methods. The currents within these ion-scale FTEs are predominantly field aligned, and are characterized by rapid fluctuations corresponding to spatial scales smaller than ion inertial length, and are called "filamentary currents" (Eastwood et al., 2016). Wang, Lu, et al. (2017) examined a sequence of three FTEs close to each other with MMS data. Two of these FTEs were characterized by filamentary currents, both parallel and perpendicular to the magnetic field, while the third FTE, which was closer to the reconnection X line, was characterized by a singular compact current layer.

The study of FTEs can be useful also to understand the processes at the X line. Indeed, one class of FTEs is associated with a "crater" signature (a local minimum or minima) in the |B| signature, which has been further subcategorized into "M"-shape and "W"-shape crater FTEs (Farrugia et al., 2011). It has been suggested that crater FTEs are related to encounters with the separatrix (Farrugia et al., 1988; Farrugia et al., 2011; Owen et al., 2008; Rijnbeek et al., 1987). Farrugia et al. (2011) in particular presented a number of signatures based on Cluster data that suggest the presence of a magnetic separatrix at the borders of a crater FTE. In particular, these authors reported the presence of an intermediate region between the FTE core and the draping region, characterized by:

1. Strong electric field fluctuations, which occur in several short burst (duration ≈ 1s) interpreted as multiple encounters with the separatrix.
2. The presence of antiparallel electrons moving toward the X line in the electron distribution function measured by the PEACE electron spectrometer, consistent with the Hall electron current. However, the sampling time of PEACE was much longer than the burst of the electric field fluctuations.
3. Fluxes of 500 eV electrons evaluated from EDI (Electron Drift Instrument) with enhancements of antiparallel electrons, that is, toward the X line, approximately at times of the electric field fluctuations.

The presence of magnetic separatrices at the borders of the FTE implies that the FTE is magnetically connected with an active X line. This excludes the original FTE model proposed by Russell and Elphic (1978), since in this model magnetic reconnection is active only during the formation of the FTE, and suggests the single or the multiple X line models. However, other interpretations of crater FTEs have been put forward. For example, Zhang et al. (2010) proposed that crater FTEs may be associated with the initial stages of formation of an FTE, and recent simulations suggest that a crater FTE may evolve into a typical FTE either due to imposed pressure perturbations (Teh et al., 2015) or once the growth of the FTE core field reaches a significant value (Chen et al., 2017).

The presence of the magnetic separatrix at the borders of an FTE was also suggested by Hwang et al. (2016), who examined the substructure of an FTE using high resolution MMS data. In particular, detailed analysis of ion and electron distribution functions suggested the presence of a thin layer separating the open FTE core field lines from the external region. This thin layer, which contains localized enhancements of electrons streaming toward the X line, together with ions emanated from the X line (See figure 3 of Hwang et al., 2016), would contain newly opened field lines connected with an active X line northward of the FTE, that is, the magnetic separatrix.

The enhanced capabilities of MMS for measuring currents allowed recently also a remarkable progress for defining the current structure in proximity of the X line, not associated with FTEs. In particular, Phan et al. (2016) demonstrated the presence of electron-scale filamentary Hall currents both near the X line region, and also in the reconnection exhaust region, further from the X line. These Hall currents were
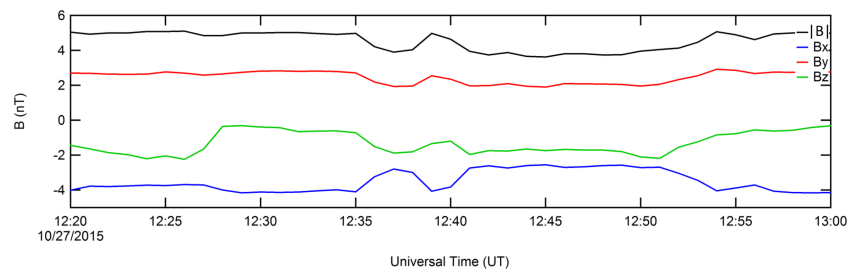
Figure 1. The orientation of the interplanetary magnetic field observed by Omni (King and Papitashvili 2004), in GSM coordinates, time-shifted to the nose of the Earth's bow shock, for the time interval of the magnetopause crossing examined in this paper.

more intense in the region near the X line, where also larger electric field fluctuations and greater electron heating were observed. Highly filamentary Hall currents in the exhaust region are predicted by various 3-D simulations (Daughton et al., 2014; Nakamura & Daughton, 2014). The fine structure of the exhaust reconnection region in proximity of the X line was also examined with MMS data by Hwang et al. (2017). They found that at/around the separatrix, large-amplitude parallel electric fields can accelerate the electrons along the separatrix, toward the X line, sustaining the Hall current system.

Here we present MMS observations of a crater FTE observed at the dayside magnetopause, which is also associated with a reconnection jets at the trailing edge, suggesting the single X line, or possibly multiple X line mechanism as the generation mechanism for this FTE (Trenchi et al., 2016). Both these models are expected to generate FTEs bounded by magnetic separatrices, magnetically connected with active reconnection X line. During prolonged time intervals, both at the leading and the trailing edge of this FTE, the high resolution MMS data observed strong fluctuations in electric field and electron velocity component parallel to the magnetic field. These intervals are characterized by stable ion velocity component, therefore the fluctuation of electron velocity give rise to currents parallel to the magnetic field carried mainly by electrons, which can be interpreted as encounters with the field aligned component of the Hall current system, along the separatrix at the borders of the FTE. The persistence of these fluctuations during extended time intervals can be due either to a filamentary structure of the Hall currents at the borders of the FTE, similar to the ones reported by Phan et al. (2016) in proximity to the X line, or rather to multiple encounters with a compact separatrix. The fact that these currents are highly attenuated in the reconnection exhaust, where both ions and electrons have similar velocities, suggests a stratification of the reconnection layer.

During this event also a jet reversal is observed a few minutes after the FTE, when MMS was probably closer to the X line. The same fluctuations were also detected in the region adjacent to these reconnection jets, confirming the hypothesis that the fluctuations were caused by encounters with a magnetic separatrix.

2. Event Overview

In this paper we examine the magnetopause crossings observed by MMS on 27 October 2015, around noon, at $(9.3, 5.9, -4.1)_{GSM}$ Re. The orientation of the IMF observed by Omni (King & Papitashvili, 2005) during this magnetopause crossing is shown in Figure 1, in GSM coordinates and time-shifted to the nose of Earth's bow shock. The IMF during this interval is stable, and it is characterized by negative B_Z and positive B_Y components.

For this study, we analyzed the magnetic field vectors measured by the Fluxgate Magnetometer (FGM; Russell et al., 2014), the ion and electron data measured by the Fast Plasma Investigation (FPI; Pollock et al., 2016), and the electric field measurements from electric field instruments, which consist of the spin-plane double probe (SDP; Lindqvist et al., 2016) and axial double probe (ADP; Ergun et al., 2014).

This magnetopause crossing is particularly useful for studying the various reconnection signatures with the high time resolution provided by MMS, because burst mode data are available during two extended time intervals, covering almost the entire event, that is, from 12:33:44 to 12:38:14 UT, and from 12:40:54 to 12:47:03 UT. In order to take the maximum advantage from the high time resolution data, we have used burst mode magnetic field data with a time resolution of 128 Hz, burst mode plasma data with a time resolution of
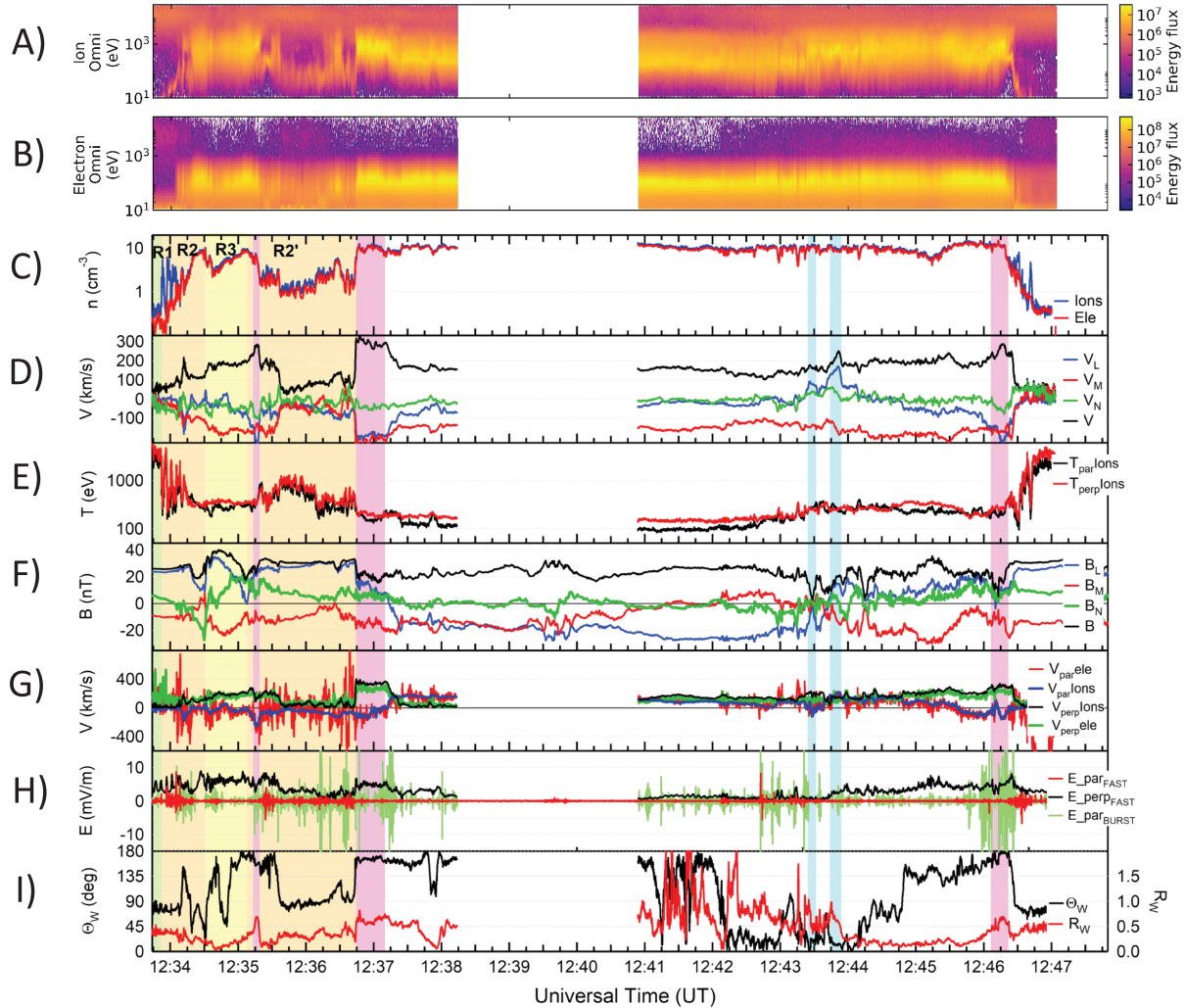
October 27, 2015

Figure 2. Overview of the MMS1 observations for the magnetopause crossing observed on 27 October 2015. (a and b) The omnidirectional differential energy fluxes of ions and electrons in spectrogram format. (c) Ion and electron density. (e) Parallel and perpendicular ion temperatures respectively. (d and f) Ion velocity vector and magnetic field components in the local boundary normal (LMN) reference frame, where N direction is outward along the local magnetopause normal, while L and M are in the plane defined by N, being northward and dawnward respectively. (g) Ion and electron velocity components parallel and perpendicular to the magnetic field direction. (h) The electric field components parallel and perpendicular to the magnetic field orientation. In panel i the two quality parameters, R_W and Θ_W are used to evaluate the agreement of the Walén relation. The green, orange and yellow shadings highlight the draping, intermediate and core FTE regions, referred to as R1, R2, and R3 using the same classification as Rijnbeek et al. (1987), while the cyan and pink shadings highlight the northward and southward reconnection jets, selected by means of the Walén relation.

30 ms for electrons and 150 ms for ions and both burst mode DCE and fast mode electric field data, with a time resolution of 8192 Hz and 30 ms, respectively.

The overview of the MMS1 observations for this event is presented in Figure 2. Figures 2a and 2b show the omnidirectional differential energy fluxes of ions and electrons in spectrogram format. At the start and end of the interval, a hot ion and electron population was observed, indicative of the spacecraft being located in the magnetosphere. Between 12:34 and 12:46 UT, the population observed was generally cooler and denser, consistent with a magnetosheath population, except for between 12:35 and 12:37 UT when the electron population was sheath-like (but lower fluxes and with the presence also of a hotter magnetospheric population) and the ion population was more magnetospheric (but with an ion population that is colder than the sheath). As will be discussed below, we interpret this period as an entry into the low-latitude boundary layer.

This spectrogram also shows the presence of a cold ion population with energies below 100 eV at the beginning and at the end of the interval, that is, before 12:34:10 UT, which is also observed after 12:46:30 UT. The spectrogram data are only plotted for the periods when the spacecraft were in burst mode and hence there is a data gap from 12:38:14 to 12:40:54 UT; however, lower cadence spectrogram data (not shown) indicate that the spacecraft was in the magnetosheath throughout this time.

In panel c of Figure 2 the ion and electron density are plotted. The two densities show a good agreement, except for the intervals when the cold ion population is detected, that is, before 12:34:10 and after 12:46:30 UT, where the ion density was lower than electron density. In panel e we show the parallel and perpendicular ion temperatures, while in panels d and f we show the ion velocity vector and the magnetic field components in the local boundary normal reference frame (LMN; Russell & Elphic, 1978). The N direction is outward along the local magnetopause normal, evaluated with the empirical Fairfield model (Fairfield, 1971), and is $(0.86; 0.41; -0.29)_{GSM}$, while L and M are in the plane defined by N, being northward and dawnward, respectively, and are $(0.26; 0.13; 0.96)_{GSM}$ and $(0.43; -0.90; 0.00)_{GSM}$. In panel g the ion and electron velocity components parallel and perpendicular to the magnetic field direction are plotted, computed from the projection of ions and electrons velocity along the magnetic field vectors measured by FGM. Given the different time resolution, for these projections, the electron velocity data and the magnetic field data have been down-sampled to the same 150-ms resolution as the ion data. In panel h we present the electric field components parallel and perpendicular to the magnetic field orientation from FAST mode data, and the parallel component from burst mode data, high-pass filtered above 20 Hz. The quality index for the electric field measurements classifies as good the majority of the electric field data measured during this interval, except at the beginning of the interval (before 12:33:50 UT), where the cold ion population is observed. During this interval, while the FAST mode electric field data could be affected by the presence of ion wake around the spacecraft, more evident at the beginning of the interval, that is, before 12:33:25 UT, the burst mode electric field data are not affected by this phenomenon, and therefore, can be considered as more reliable.

Before 12:34:00 UT, MMS was in the magnetosphere proper, characterized by low density, high temperature, and a stable magnetic field oriented along positive L and negative M direction. From 12:33:30 to 12:36:10 UT, MMS detected a large FTE characterized by a negative-positive B_N signature, and also a clear signature in the magnetic field intensity; this corresponds to the first period of observation of magnetosheath-energy plasma (panels a and b) which we interpret as entry of plasma on open field lines. The polarity of the B_N signature implies that the spacecraft is southward of the X line.

This is further confirmed by the spectrograms reported in Figure 3, which present an enlargement about the FTE with the same format as Figure 2, where the ion and electron omnidirectional fluxes are restated (panels a and b), and the electron populations observed parallel (panel b1), antiparallel (panel b2), and perpendicular (panel b3) to the magnetic field are shown for the interval corresponding to the entry of MMS into this FTE. This spectrogram demonstrates that the magnetosheath energy plasma was observed first antiparallel (and perpendicular) to the magnetic field, and then parallel. The observation of magnetosheath antiparallel electrons before the parallel magnetosheath electrons is consistent with being on open field lines connected to the southern hemisphere, which is also consistent with the negative – positive B_N signature. The subsequent appearance of the parallel population is consistent with electrons mirroring and returning towards the magnetopause. According to Vaivads et al. (2010), the location of the magnetic separatrix at the leading edge of the FTE can be identified from particle data as the boundary where high energy magnetospheric electrons (with energies larger than 1 keV) moving away from the X line disappear. In this case, given that MMS is southward of the X line when the FTE is observed, we identified the separatrix at the leading edge of the FTE from the antiparallel electrons, shown in panel B2 of Figure 3. With this criterion, the first encounter with the magnetic separatrix at the leading edge of the FTE is observed at 12:34:03, indicated by black line in Figure 3. Later on during the FTE interval, the fluxes of high energy antiparallel electrons show several other intensifications (e.g., at 12:34:20, 12.34.30, 12:35:40, and 12:35:55 UT, see the black shaded boxes in panel b2), which could be related to other encounters with magnetic separatrices.

MMS was located in the magnetosphere proper before the FTE, instead at the trailing edge of the FTE, from 12:35:10 to 12:36:45 UT; it returned in the magnetospheric side of the low-latitude boundary layer. This is indicated by the combination of a magnetosheath-energy electron population (with differential energy fluxes lower than in the magnetosheath proper) and a higher energy magnetospheric electron population (seen
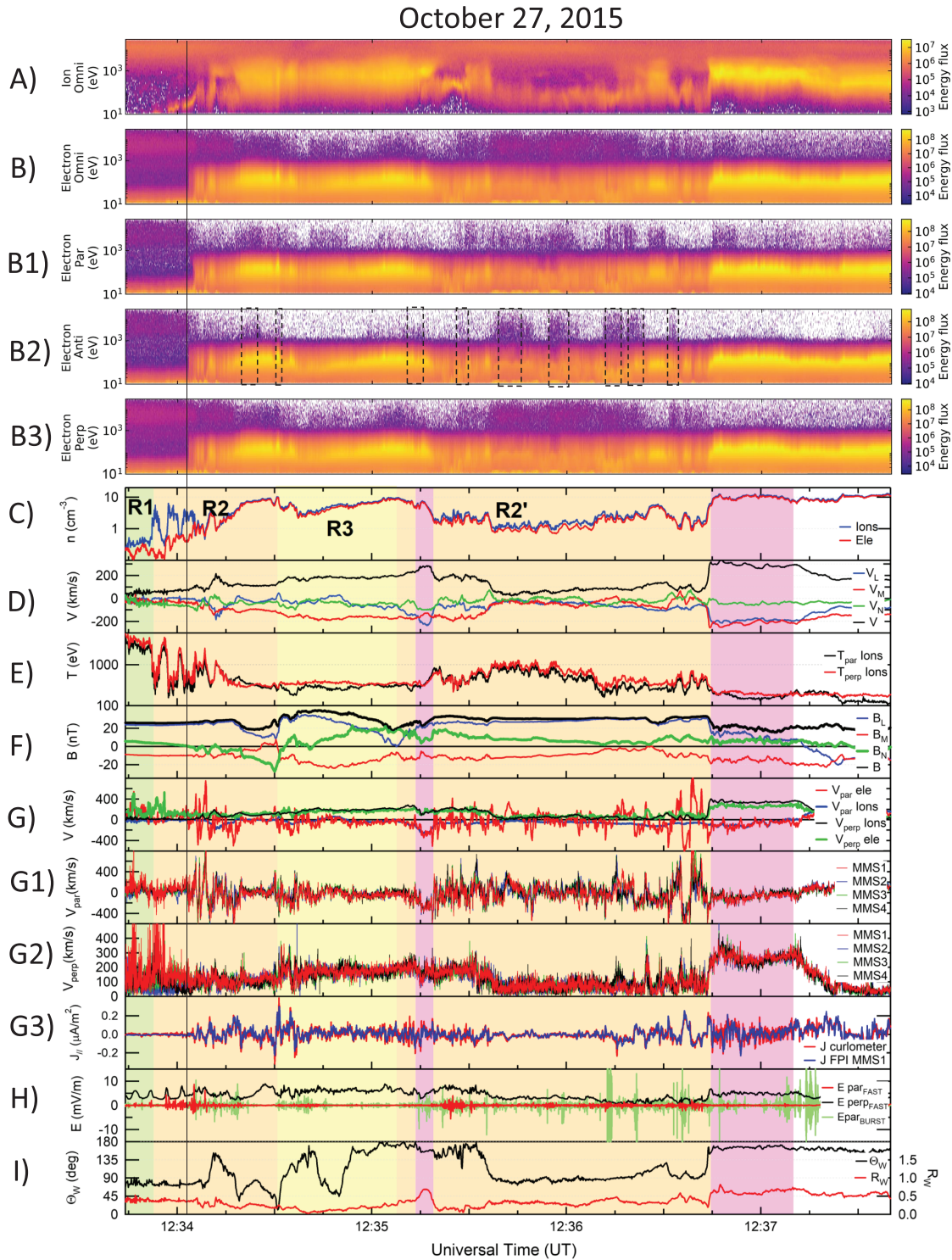
Figure 3. An enlargement about the flux transfer event (FTE), with the same format as Figure 2. The additional spectrograms in panels b1, b2, and b3 show the electron populations observed parallel to the magnetic field (b1), antiparallel to the magnetic field (b2) and perpendicular to the magnetic field (b3). The additional panels g1 and g2 show the parallel and perpendicular components of the electron velocity measured by the four MMS spacecraft, while the additional panel g3 illustrate a comparison between the parallel currents obtained from plasma data, and from magnetic field data estimated from the curlometer technique. The green, orange, and yellow shadings highlight the draping, intermediate and core FTE regions (R1, R2, and R3), while the cyan and pink shadings highlight the northward and southward reconnection jets, selected by means of the Walén relation. The black line indicates the first encounter with the magnetic separatrix at the leading edge of the FTE, while the black shaded boxes in panel B2 highlight the enhancements of high energy antiparallel electrons, which can be due to other encounters with magnetic separatrices.

most clearly in the pitch angles perpendicular to the magnetic field; panel b3). The ion population (Figures 3a and also 2a) are also more consistent with a magnetospheric population, though a cold ion population is observed. This means that this FTE can be classified as a magnetospheric FTE. Moreover, in analogy with the magnetospheric crater FTEs examined by Farrugia et al. (1988), this FTE is characterized by a maximum of the magnetic field intensity at the FTE center, identified as the time interval where the B_N is approximately zero, flanked by two local minima in the magnetic field intensity; this makes it a "W"-shape crater FTE (Farrugia et al., 2011).

It has been noted that these crater FTEs are generally characterized by a stratification of three distinct regions (Rijnbeek et al., 1987), which are the draping region in the external part (R1), the core region formed by open reconnected field lines (R3), and an additional intermediate region (R2), where the density and temperature change gradually from the magnetospheric to the magnetosheath values and vice versa, which has been suggested to contain newly open field lines connected with an active reconnection X line, that is, the separatrices (see also Farrugia et al., 1988, 2011). The draping, intermediate, and core regions are referred to as R1, R2, and R3 and are crossed in reverse order as the spacecraft exits the FTE. In Figure 2, we used the same classification proposed by Farrugia et al. (2011), based on magnetic field and ion data, using the green, orange and yellow shadings to identify the draping (R1 and R1′), intermediate (R2 and R2′) and core (R3) regions, respectively. We use the notation R2′ to refer to the intermediate region encountered as MMS1 was outbound from the FTE, and we note that the outbound draping region R1′ is probably not detected after this FTE, since MMS remained in the boundary layer and did not enter the magnetosphere proper after the FTE. For this reason, the extent of R2′ on the trailing edge of the FTE is chosen according to the B_N signature, which is somewhat arbitrary. After the FTE, MMS crossed the magnetopause at around 12:37 UT (indicated by a reversal in B_L which also corresponds to the transition seen in the spectrograms from LLBL to magnetosheath), and remained in the magnetosheath until around 12:43 UT (Figure 2). Between 12:43 and 12:46 UT, the spacecraft observed a heated magnetosheath population (Figures 2a and 2b) and a reversal in B_L back to a northward orientation (Figure 2f), consistent with an inbound magnetopause crossing back through a boundary layer structure until the magnetosphere-proper was observed (after 12:46 UT).

During this interval, a number of periods of fast flow were observed (Figure 2d). In order to identify reconnection jets, we performed the Walén test in the spacecraft reference frame taking into account the plasma anisotropy (Hudson, 1970), which has been successfully applied in several statistical studies of magnetic reconnection at the magnetopause (Paschmann et al., 1986; Phan et al., 1996; Trenchi et al., 2008; Trenchi et al., 2009). This test consists of the comparison of the observed velocity jump relative to a reference value in the magnetosheath $V-V_{\mathrm{MSH}}$ with the expected velocity jump ΔV_{th} predicted by the Walén relation (equation (1) of Trenchi et al., 2008, 2011, 2016). For this event, the magnetosheath reference period is chosen from 12:41:00 to 12:42:00 UT. Comparing these two vectors, we obtained R_W as the ratio of their absolute values, and Θ_W as their relative angle, which are shown in panel i) of Figure 2. The Walén test is perfectly fulfilled when R_W equals unity and Θ_W equals 0° or 180°, corresponding to the positive or negative signs of the Walén relation that, at the dayside magnetopause, correspond to observations northward or southward of the X line. Here we consider that the Walén relation is satisfied when $0.4 < R_W < 3$, and $\Theta_W < 30°$ or $\Theta_W > 150°$, for at least three consecutive data points, with average ion density larger than 1 cm^{-3} (Trenchi et al., 2008, 2011, 2016). The northward and southward reconnection jets selected by means of the Walén relation are highlighted by cyan and pink shadings in Figure 2.

It can be noted that in region R2′ of the FTE the Walén relation indicates the presence of a southward reconnection jet at 12:35:15 UT, soon after the FTE center; another southward reconnection jet is observed at 12:37:00 UT, soon after the FTE (and coinciding with the magnetopause crossing). These jets are moving in the same direction of the FTE, and the first one is observed at its trailing edge. This feature suggests the single X line, or possibly the multiple X line mechanism (with a dominant X line) as the generation mechanism of this FTE (Trenchi et al., 2016). The electron signatures in the spectrogram are also consistent with the single X line model: the presence of magnetosheath-energy electrons moving antiparallel to the magnetic field before parallel electrons are observed (spectrograms in Figure 3) is consistent with open field lines connected to the southern hemisphere. Although we do not observe any evidence for converging jets either side of the FTE (Trenchi et al., 2011), the observations could alternatively be

consistent with a multiple X line formation if reconnection at the northern X line is dominating, and the spacecraft does not enter deeply enough into the FTE to see directly the effects of the secondary X line (Trenchi et al., 2016).

Around 12:44:00 UT other reconnection jets have been identified, which are directed northward around 12:43:30 UT, and then a southward reconnection jet at 12:46:00 UT. These jets can be interpreted as a jet reversal event, indicating the passage of the X line in proximity of MMS, and coincide with the boundary layer structure observed around the magnetopause crossing at 12:43:00–12:46:00 UT, and will be discussed later in Section 4.

3. High-Resolution Particle Observations of a Crater FTE

In Figure 3, which presents an enlargement about the FTE with the same format as Figure 2, the additional panels G1 and G2 show the comparison of the parallel and perpendicular electron velocities observed by the four MMS, while the additional panel G3 illustrates a comparison between the parallel current densities obtained from plasma data, and from magnetic field data estimated with the curlometer technique. At the borders of this FTE, in region R2 and R2′, more precisely during prolonged time intervals around 12:34:05 and after 12:35:20 UT, the electric field components (panel h) show high-frequency fluctuations, involving mainly the parallel electric field component. These fluctuations of the parallel electric field component are highly attenuated inside the FTE core, are more intense in region R2, and occur also in region R2′ at the trailing edge of the FTE, with lower amplitudes until 12:36:45. These electric field fluctuations, which are similar to the electric field fluctuations reported by Farrugia et al. (2011) in the intermediate region R2, can be interpreted as due to encounters with a magnetic separatrix surrounding the FTE (Farrugia et al., 2011; Retinò et al., 2006; Wilder et al., 2016). This interpretation is confirmed by the fact that these electric field fluctuations are highly attenuated also during the time intervals selected as reconnection jets (pink shading). Indeed, due to time of flights effects in the reconnection layer, the accelerated particles forming the reconnection jets can be observed only in the more internal part of the reconnection layer (Lockwood et al., 1996). This point will be far enough from the separatrix, so that the signatures of the separatrix are absent during the jets.

In regions R2 and R2′, approximately at the same time intervals of these electric field fluctuations, several fluctuations of the parallel electron velocity component were observed, both with positive and negative signs (panel G). The amplitudes of these fluctuations exceeded 500 km/s, and have time scales shorter than one second (hence such velocity fluctuations would not be detectable by plasma instruments on previous spacecraft missions). These parallel electron velocity fluctuations are most intense at the beginning of R2, soon after the reconnection jet at 12:35:15, and before the jet at 12:37 UT. It should be noted that these fluctuations of the electron velocity involve only the parallel velocity component, while the perpendicular electron velocity component matches remarkably well the perpendicular ion velocity component during the entire interval, and the ion parallel velocity component remains stable, indicating that these signatures correspond to parallel current fluctuations. As with the electric field fluctuations, the fluctuations of parallel electron velocity component are significantly attenuated during both intervals selected as reconnection jets (pink shadings). Indeed, during the two reconnection jets, the parallel component of electron velocity matches remarkably well the parallel component of ion velocity.

To rule out the possibility that these fluctuations are artifacts of the instrumentation aboard MMS1, we compared the parallel and perpendicular electron velocity components measured by all the other MMS spacecraft in panels g1 and g2 in Figure 3. All the four spacecraft detected very similar fluctuations of the parallel component of the electron velocity (panel g1). This suggests that the observed fluctuations of the electron velocity are caused by some real physical effect in this region, which has a spatial scale larger than the separation of the MMS spacecraft (approximately 10 km during this event). As a further test, we computed the parallel current density from ion and electron velocities measured by FPI on MMS1 as $J_\parallel = nq$ $(V_i - V_e)$, where n is the electron density, q is the elementary charge of proton, and V_i and V_e the velocity of ions and electrons, respectively (Eastwood et al., 2016). In panel G3 we compare this parallel current density obtained from FPI with the parallel current density computed via the curlometer method (Dunlop et al., 2002; Robert et al., 1998). We can note that the two current densities show a very good agreement during this interval, confirming the real nature of these electron velocity fluctuations.

4. The Reconnection Jet Reversals

Figure 4 presents an enlargement about the reconnection jets observed in the last part of the event, with the same format as Figure 3.

At the start of the interval displayed in Figure 4, MMS was observing the magnetosheath proper, where all the parameters displayed in Figure 4 show a smooth and stable behavior. Only the perpendicular component of the electric field shows some periodic oscillations before 12:42 UT, with a time period of approximately 5 seconds (panel h). Therefore, these oscillations have different features with respect to the fluctuations discussed in the previous paragraph, since they involve mainly the perpendicular component, and are characterized by a much lower frequency.

The northward reconnection jets observed around 12:43:30 UT suggest that MMS is now northward of the X line. The magnetic separatrix is therefore identified as the first encounter with magnetospheric electrons moving away from the X line, from the parallel electrons spectrogram (Vaivads et al., 2010). The separatrix is observed at 12:42:07 UT, and it is indicated by the black line in Figure 4.

After the magnetic separatrix in the boundary layer, MMS observes similar behavior to that seen in region R2 and R2′ of the FTE. At this time, both the parallel and perpendicular components of the electric field (panel h) show some high-frequency oscillations, with smaller amplitudes respect to the ones discussed previously, and the parallel electron velocity component starts to oscillate (panel g). These fluctuations of the parallel velocity component have smaller amplitude with respect to the ones discussed in the context of the FTE, but are continuously observed in the entire interval after 12:42:15 (once the spacecraft has entered the boundary layer; panel b). Also, in this case, all four MMS spacecraft detect very similar fluctuations of the parallel component of the electron velocity (panel g1), and the parallel current densities estimated from plasma data and from curlometer technique agree well (panel g3). Again, the fluctuations of electric field and parallel electric velocity component appear to be highly attenuated during both the northward reconnection jets, with some intensification of the fluctuations of parallel electron velocities just before the northward reconnection jets at 12:43:15.

The detection of the two northward reconnection jets around 12:43:30 to 12:44:00 UT (cyan shadings), implies that during these jets MMS has penetrated into the reconnection layer, as also deduced from the spectrograms in the first two panels. In particular, during the second northward reconnection jet, observed at 12:43:50 UT, MMS was in the magnetospheric side of the reconnection layer, as deduced by the positive sign of B_L. This implies that in the time interval preceding these jets, MMS should have crossed the magnetic separatrix, and penetrated into the reconnection layer, crossing the magnetopause. The electric field and parallel electron velocity fluctuations detected in the time interval 12:42:10 – 12:43:20 UT could therefore be caused by the encounter with the magnetosheath magnetic separatrix northward of the X line.

During the time interval 12:44:00 – 12:46:00 UT, MMS remained in the boundary layer, as deduced by the simultaneous presence of magnetosheath and magnetospheric ions in the spectrograms. The spacecraft remained on the magnetospheric side of the magnetopause as deduced from the positive B_L, while the IMF remained constantly southward during this interval (Figure 1). During this interval, high-frequency fluctuations of the parallel electron velocity component are detected continuously, although with smaller intensity. This suggests that MMS is remaining near the magnetospheric separatrices.

Around 12:46:15 UT, MMS detects a southward reconnection jet, and then after 12:46:30 UT, it leaves the boundary layer and enters the magnetosphere-proper. The passage from northward to southward reconnection jets during this interval could be explained by a northward motion of the X line, which would be expected according to the diamagnetic drift effect, given the positive IMF B_Y component (see Figure 1 of Trenchi et al., 2015). Alternately, this passage could be explained by an FTE generated by multiple X line reconnection sites travelling southward, and the observed reconnection jets would be the converging jets expected at the borders of the FTEs generated by multiple reconnection X lines (Hasegawa et al., 2010; Trenchi et al., 2011). In fact, in the interval 12:44:48–12:45:50 (see panel F of Figure 4), MMS observed an intensification of the B_M component, associated with an extremely weak and extended negative-positive bipolar signature in the B_N component, although not symmetric about B_N=0, which could indicate the presence of a second FTE moving southward. However, the four-spacecraft timing technique does not confirm
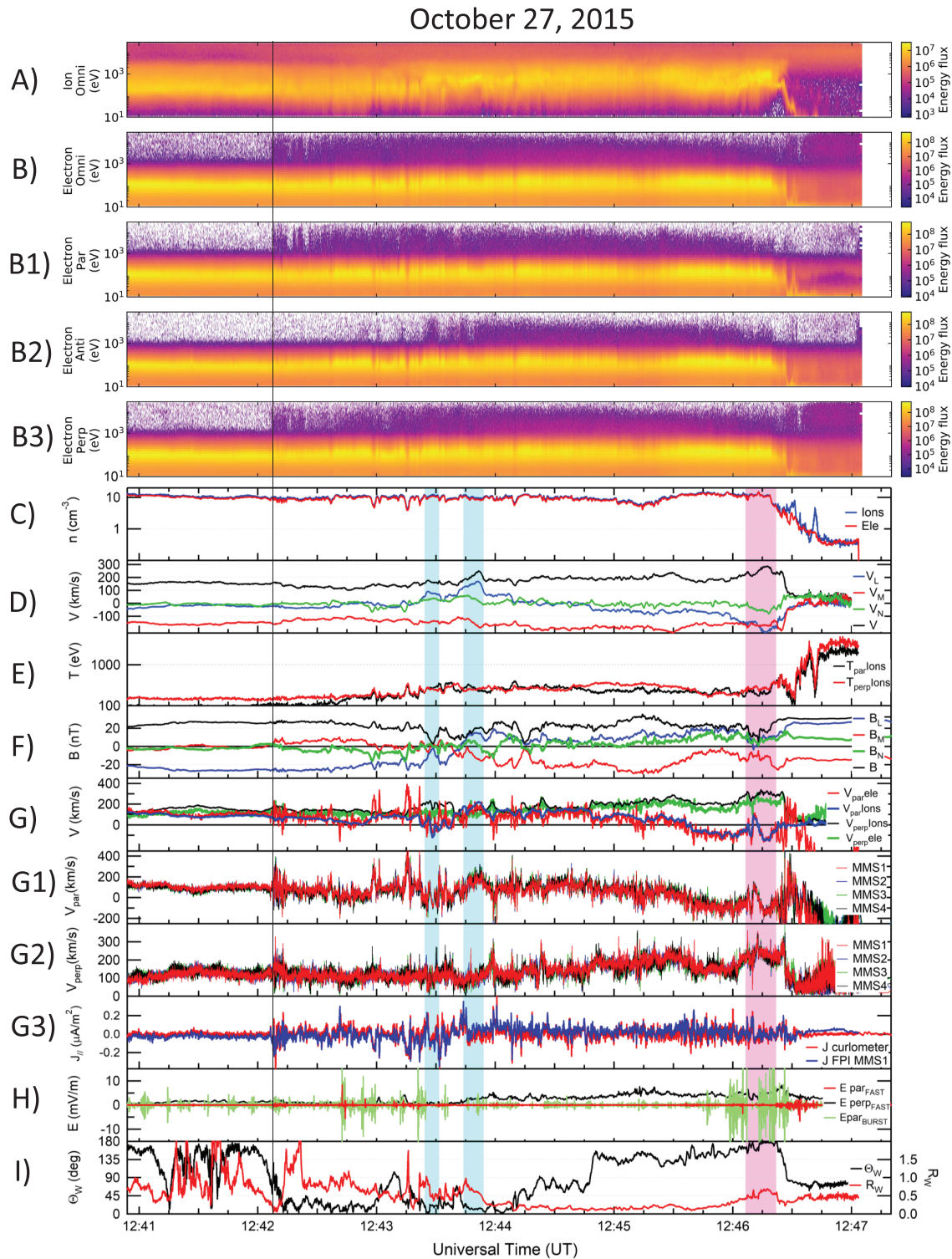
Figure 4. An enlargement about the reconnection jets observed in the last part of the event, with the same format as Figure 3. The cyan and pink shadings highlight the northward and southward reconnection jets, selected by means the Walén relation. The black line indicates the magnetic separatrix.

that this is a coherent structure moving southward. Instead, when applying this method to various intervals within this structure, we obtained different velocities (not shown). The velocity of this structure obtained with the deHoffmann Teller analysis has a negligible southward component, and it is essentially along negative M, such as the magnetosheath velocity (not shown). Therefore, we cannot confirm which scenario
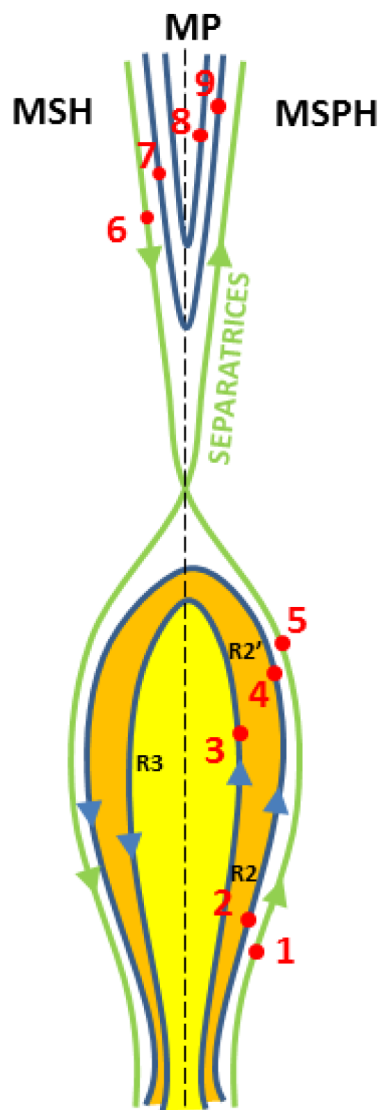
Figure 5. A schematic of the flux transfer event which includes the structure of the reconnection layer as inferred from our observations.

(i.e. single X line moving northward, or FTE generated by multiple X lines moving southward) was responsible for the jet reversal during this interval.

Also during the southward reconnection jet, the fluctuations of the parallel electron velocity are further reduced in amplitude, while these fluctuations appear again after the jet (after 12:46:20 UT), with increased amplitudes, when also high-frequency fluctuations of the parallel electric field component with increased amplitude are detected (panel h). These fluctuations can be therefore interpreted as due to other encounters with the magnetospheric separatrix southward of an X line.

In the last part of the event (after 12:46:30 UT) the parallel electron velocity component shows a large and stable deviation with respect to the ion parallel velocity. We speculate here that this deviation could be due to some instrumental issues.

5. Discussion

In this paper, we reported a magnetopause crossing characterized by the presence of a crater FTE, and reconnection jets, based on high time resolution MMS plasma and field data. This event in particular is very useful to study the reconnection layer with high definition, since the burst mode data are available during two extended time intervals, covering almost the entire event.

In Figure 5, a schematic of the FTE which includes the structure of the reconnection layer as inferred from our observations, is shown.

At the borders of the FTE, in the intermediate regions between the FTE core and the draping regions (Points 1, 2 and 4, 5 respectively, in Figure 5), we detected during prolonged time intervals several high-frequency fluctuations of the parallel electric field component, which were attenuated in the FTE core, during the reconnection jet at the trailing jet of the FTE and in the magnetosheath intervals. Similar fluctuations were already reported at the borders of a crater FTE by Farrugia et al. (2011), and were interpreted as due to multiple encounters with the magnetic separatrix.

We found that these electric field fluctuations are associated with strong positive and negative fluctuations of the component of the electron velocity parallel to the magnetic field. These fluctuations are similar among all the four MMS spacecraft, and involve only the parallel component of electron velocity since the perpendicular components of ion and electron velocities remain always in a good agreement. These fluctuation of electron velocity give rise to currents parallel to the magnetic field, carried mainly by electrons, since the parallel component of the ion velocity is more stable. The high time resolution MMS burst mode data were crucial to highlight this behavior of the electron velocity in these regions, since the frequency of these fluctuations is higher than 1 Hz, so that these fluctuations would not be detectable by plasma instruments onboard previous missions, characterized by much lower time resolution.

These positive and negative fluctuations of parallel electron velocity component (and field-aligned currents) can be due to encounters with the magnetic separatrix and the reconnected field lines adjacent to it at the borders of this FTE.

Indeed, it is expected that along the separatrices the electrons flow toward the X line, having a larger parallel velocity with respect to ions, sustaining the field aligned component of the Hall current system. In the case of the present observations, MMS is located southward of the X line, as deduced by the FTE polarity, by the presence of southward reconnection jet and by the anisotropy of the magnetosheath-energy electrons observed on entry to the FTE at 12:34:00 UT (see the black line in Figure 3) between the parallel and antiparallel
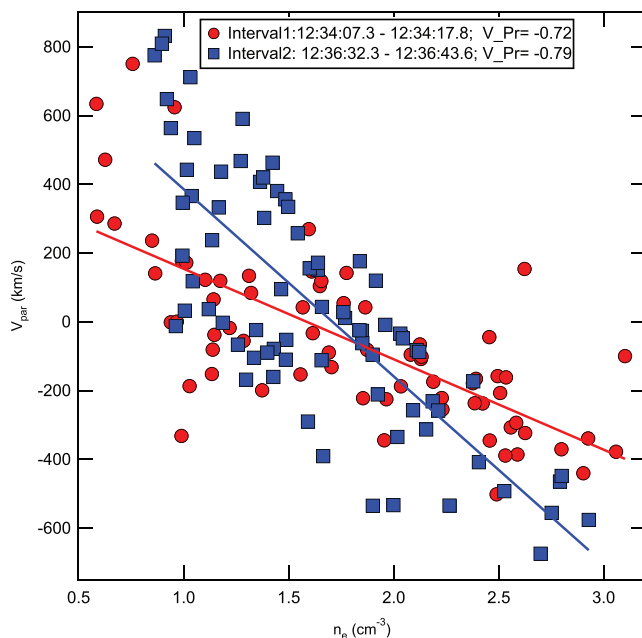
Figure 6. A scatter plot of parallel electron velocity component as a function of the electron density, measured by MMS1, in the two intervals at the borders of the flux transfer event characterized by stronger fluctuations of parallel electron velocity at the borders of the flux transfer event, together with the linear fits.

magnetosheath populations. Furthermore, MMS was on the magnetospheric side of the magnetopause, as deduced by the positive B_L component and the magnetospheric/LLBL plasma populations observed immediately before and after the FTE, respectively. Therefore, the electrons moving toward the X line are the ones with positive parallel velocity, and all the positive fluctuations of the parallel electron velocity can be interpreted as due to the electrons flowing toward the X line along the separatrices (points 1 and 5 in Figure 5, for regions R2 and R2′, respectively).

Also the negative fluctuations of parallel electron velocity can be due to encounters with the separatrices, and reconnected field lines adjacent to them. Indeed, according to the simulations of Wang et al. (2010) and Zenitani and Nagai (2016), in proximity of the X line, the electrons flowing toward the X line are reflected back along the field lines, and then accelerated by the reconnection electric field near the X line. These electrons would then flow away from the X line along the reconnected field lines adjacent to the separatrices. It has to be noted, however, that these simulations adopt a symmetric plasma density profile across the current sheet, which is not representative of the conditions of reconnection at the magnetopause. Other simulations reporting the electron behavior around the separatrices for asymmetric reconnection representative for the magnetopause conditions, are reported by Pritchett (2008) and Zenitani et al. (2017). Pritchett (2008) reported a substantial flux of parallel electrons moving toward the X line along the magnetospheric separatrices, while along the reconnected field lines adjacent to the magnetospheric separatrices the electrons were moving away from the X line (see Figure 8 d) of Pritchett (2008)). In these simulations, however, these electrons moving away from the X line adjacent to the magnetospheric separatrix would be mostly of magnetosheath origin, that is, electrons penetrating from the magnetospheath, rather than electrons reflected at the X line.

Therefore, the negative fluctuations of the parallel electron velocity observed at the borders of the FTE (regions R2 and R2′) can be explained as being due to these electrons flowing away from the X line, along the reconnected field line adjacent to the southward magnetospheric separatrix (Points 2 and 4 for regions R2 and R2′, respectively).

As a test of the hypothesis that these fluctuations are due to encounters with the magnetic separatrix layer, we displayed in the scatterplot in Figure 6 the parallel electron velocity component as a function of electron density, measured by MMS1, in the two intervals at the borders of the FTE characterized by stronger fluctuations of parallel electron velocity at the borders of the FTE, that is, 12:34:07 – 12:34:17 UT and 12:36:32 – 12:36:44 UT. As mentioned before, the simulations predict an electron flow moving toward the X line along the magnetospheric separatrices, and another electron population moving away from the X line along the reconnected field lines adjacent to them. In case of asymmetric reconnection (Pritchett, 2008), also a density gradient is present at the magnetospheric separatrices, therefore, a negative correlation between parallel electron velocity and electron density is expected in proximity of the southward magnetospheric separatrix (panels b) and d) in figure 8 of Pritchett, 2008). From Figure 6, these two quantities show a clear and negative correlation, which is statistically significant since the correlation coefficients of the linear fits (indicated by V_Pr in the figure) are larger than 0.7. This confirms that MMS observed magnetospheric separatrices at the borders of this Crater FTE.

In these intervals, the multiple repetitions of positive and negative fluctuations of parallel component of electron velocity can be due either to multiple encounters with a compact separatrix, or alternatively to a filamentation of the separatrix current layer, as observed by Phan et al. (2016) in proximity to the X line.

In this regard, we note that brief and intermittent encounters with magnetosheath populations are also evident in the parallel-antiparallel-perpendicular electron spectrograms shown in Figure 3. In particular, this intermittent behavior is more evident in the antiparallel & perpendicular spectrograms shown in panels

B2 and B3 during both intermediate regions surrounding the FTE core R2 and R2′. This feature supports the idea of multiple encounters with a compact separatrix during these intervals, which in turn can be related to a back and forth motion of the magnetic separatrix, or rather to some kind of ripples in the separatrix surface.

We performed the multispacecraft timing analysis described by the technique described by Harvey (1998) to further investigate the motion of the separatrix current layer. In particular, we used the simple boundary crossing technique illustrated by Harvey (1998, p 308), and we examined several separatrix current sheet crossings, where the more evident fluctuations of parallel electron velocity component are observed (not shown). We found that the velocity of the current sheet with respect to the MMS tetrahedron do not reverse the normal component between consecutive crossings, contrarily to what expected if the multiple crossings are caused by a back and for motion of the current sheet. Therefore, our observations suggest that the multiple crossings of the magnetic separatrices are due to ripples in the current sheet.

The fact that these fluctuations of parallel electron velocities are highly attenuated during the reconnection jets suggests a stratification of the particles in the reconnection layer, where electrons are flowing toward the X line along the separatrix, electrons are flowing away from the X line along the reconnected field lines adjacent to the separatrices, and ions and electrons forming the reconnection jets are flowing away from the X line with similar velocities, more internally in the reconnection layer.

This behavior is confirmed by the MMS observations during the jet reversal, when MMS passed from northward to southward of the X line. Indeed, the high-frequency fluctuations of the electric field and of the parallel component of the electron velocity are absent during the magnetosheath interval, and then start simultaneously just before the northward reconnection jets observed at 12:43:30 UT (see Figure 4), when the spacecraft is more probably crossing the northward magnetosheath separatrix (point 6 in Figure 5) and the reconnected field line adjacent to it (point 7 in Figure 5). These fluctuations are then again attenuated during the northward reconnection jet (points 8 and 9 in Figure 5). After that, the spacecraft is moving southward with respect to the X line, remaining probably nearby the northward and then southward magnetospheric separatrices, continuing to detect these fluctuations of electric field and parallel electron velocity, even if with smaller amplitudes. A northward motion of the X line is expected during this event given the positive IMF B_Y component, according to the diamagnetic drift effect (Trenchi et al., 2015). After the southward reconnection jet detected around 12:46:15 UT (see Figure 4) an intensification of fluctuations of parallel electric field and electron velocity components is observed, probably in correspondence with the southward magnetospheric separatrix (similar to point 5 in Figure 5, even though the bipolar perturbation indicating the presence of the FTE structure is not observed).

6. Conclusions

We have presented here MMS observations of a crater FTE, characterized by a reconnection jet at its trailing edge. This feature suggests the single X line, or possibly the multiple X line mechanism (with a dominant X line) as the generation mechanism of this FTE (Trenchi et al., 2016). We used the highest time resolution burst mode MMS data, that in this event are available during two extended intervals, covering almost the entire event. These high resolution MMS data allowed a detailed study of the FTE and the surrounding reconnection layer.

During extended time intervals before and after the FTE core, we observed strong fluctuations in components of electric field and electron velocity parallel to the magnetic field. These fluctuations are observed only at the borders of the FTE, since they are absent in the FTE core, during the reconnection jet at the trailing edge of the FTE and during the other magnetosheath or magnetosphere intervals.

While similar fluctuations in the electric field were also reported by Farrugia et al. (2011), the fluctuations of the parallel electron velocity component at the borders of the crater FTE were reported for the first time in this paper. Indeed, these fluctuations are observed at time scales shorter than 1 second, so that they were not detectable by plasma instruments on previous missions.

We interpreted these fluctuations as due to the presence of the magnetic separatrix connected with an active reconnection X line at the borders of the FTE. The relative motion of electrons and ions generate parallel currents, which would be the signature of the field aligned component of the Hall current system around the FTE. Electrons are expected to flow toward the X line along the separatrix, and away from the X line

along the reconnected field line adjacent to the separatrix (Nagai et al., 2003; Wang et al., 2010; Zenitani & Nagai, 2016).

At the borders of the FTE, these positive-negative fluctuations in the parallel electron velocity component are observed repeatedly during extended time intervals. The repetition of these fluctuations can be explained by multiple encounters with a compact magnetic separatrix as suggested by Farrugia et al. (2011), or rather by a filamentation of the currents in the separatrix region (Phan et al., 2016). Our observations are more in agreement with the former hypothesis, since in these intervals also the magnetosheath population is encountered intermittently (see the electron spectrograms in Figure 3, panels B2 and B3). Similar fluctuations are observed also during following encounters with magnetic separatrices, adjacent to the other intervals selected as reconnection jets.

The presence of the magnetic separatrix connected with an active X line at the borders of this FTE suggests that the FTE is formed by the single X line generation mechanism. Our observations indeed suggest a stratification of the reconnection layer forming the FTE, analogous to the one predicted by the single X line model. Given the similarities of the signatures observed in the electron velocity by the four MMS spacecraft, it seems that the spatial separation between these different reconnection layers is larger than the MMS separation during this event (which was approximately 10 km). Further statistical studies are needed to confirm this stratification of the reconnection layer inside the FTEs.

References

Burch, J. L., Moore, T. E., Torbert, R. B., & Giles, B. L. (2015). Magnetospheric Multiscale overview and science objectives. *Space Science Reviews*, 1–17. https://doi.org/10.1007/s11214-015-0164-9

Burch, J. L., Torbert, R. B., Phan, T. D., Chen, L. J., Moore, T. E., Ergun, R. E., et al. (2016). Electron-scale measurements of magnetic reconnection in space. *Science*, *352*(6290), aaf2939. https://doi.org/10.1126/science.aaf2939

Chen, Y., Tóth, G., Cassak, P., Jia, X., Gombosi, T. I., Slavin, J. A., et al. (2017). Global three-dimensional simulation of Earth's dayside reconnection using a two-way coupled magnetohydrodynamics with embedded particle-in-cell model: Initial results. *Journal of Geophysical Research: Space Physics*, *122*, 10,318–10,335. https://doi.org/10.1002/2017JA024186

Daughton, W., Nakamura, T. K. M., Karimabadi, H., Roytershteyn, V., & Loring, B. (2014). Computing the reconnection rate in turbulent kinetic layers by using electron mixing to identify topology. *Physics of Plasmas*, *21*, 052307. https://doi.org/10.1063/1.4875730

Dungey, J. W. (1961). Interplanetary magnetic field and auroral zones. *Physical Review Letters*, *6*, 47–48. https://doi.org/10.1103/PhysRevLett.6.47

Dunlop, M. W., Balogh, A., Glassmeier, K.-H., & Robert, P. (2002). Four-point Cluster application of magnetic field analysis tools: The curlometer. *Journal of Geophysical Research*, *107*(A11), 1384. https://doi.org/10.1029/2001JA0050088

Eastwood, J. P., Phan, T. D., Cassak, P. A., Gershman, D. J., Haggerty, C., Malakit, K., et al. (2016). Ion-scale secondary flux ropes generated by magnetopause reconnection as resolved by MMS. *Geophysical Research Letters*, *43*, 4716–4724. https://doi.org/10.1002/2016GL068747

Eastwood, J. P., Phan, T. D., Øieroset, M., & Shay, M. A. (2010). Average properties of the magnetic reconnection ion diffusion region in the Earth's magnetotail: The 2001-2005 Cluster observations and comparison with simulations. *Journal of Geophysical Research*, *115*, A08215. https://doi.org/10.1029/2009JA014962

Ergun, R. E., Tucker, S., Westfall, J., Goodrich, K. A., Malaspina, D. M., Summers, D., et al. (2014). The axial double probe and fields signal processing for the MMS mission. *Space Science Reviews*, *199*(1-4), 167–188. https://doi.org/10.1007/s11214-014-0115-x

Fairfield, D. H. (1971). Average and unusual locations of the Earth's magnetopause and bow shock. *Journal of Geophysical Research*, *76*, 6700–6716.

Farrugia, C. J., Chen, L. J., Torbert, R. B., Southwood, D. J., Cowley, S. W. H., Vrublevskis, A., et al. (2011). "Crater" flux transfer events: Highroad to the X line? *Journal of Geophysical Research*, *116*, A02204. https://doi.org/10.1029/2010JA015495

Farrugia, C. J., Lavraud, B., Torbert, R. B., Argall, M., Kacem, I., Yu, W., et al. (2016). Magnetospheric Multiscale Mission observations and non-force free modeling of a flux transfer event immersed in a super-Alfvénic flow. *Geophysical Research Letters*, *43*, 6070–6077. https://doi.org/10.1002/2016GL068758

Farrugia, C. J., Rijnbeek, R., Saunders, M., Southwood, D., Rodgers, D., Smith, M., et al. (1988). A multi-instrument study of flux transfer event structure. *Journal of Geophysical Research*, *93*, 14,465–14,477.

Fear, R. C., Milan, S. E., Fazakerley, A. N., Lucek, E. A., Cowley, S. W. H., & Dandouras, I. (2008). The azimuthal extent of three flux transfer events. *Annales de Geophysique*, *26*(8), 2353–2369. https://doi.org/10.5194/angeo-26-2353-2008

Fear, R. C., Trenchi, L., Coxon, J. C., & Milan, S. E. (2017). How much flux does a flux transfer event transfer? *Journal of Geophysical Research: Space Physics*, *122*, 12,310–12,327. https://doi.org/10.1002/2017JA024730

Fujimoto, M., Nakamura, M. S., Shinohara, I., Nagai, T., Mukai, T., Saito, Y., et al. (1997). Observations of earthward streaming electrons at the trailing boundary of a plasmoid. *Geophysical Research Letters*, *24*, 2893–2896.

Harvey, C. C. (1998). Spatial gradients and the volumetric tensor. In G. Paschmann and P. W. Daly (Eds.). *Analysis Methods for Multi-Spacecraft Data* (pp. 307–348). ISSI.

Hasegawa, H., Wang, J., Dunlop, M. W., Pu, Z. Y., Zhang, Q. H., Lavraud, B., et al. (2010). Evidence for a flux transfer event generated by multiple X-line reconnection at the magnetopause. *Geophysical Research Letters*, *37*, L16101. https://doi.org/10.1029/2010GL044219

Hudson, P. D. (1970). Discontinuities in an anisotropic plasma and their identification in the solar wind. *Planetary and Space Science*, *18*, 1611–1622.

Hwang, K.-J., Sibeck, D. G., Choi, E., Chen, L. J., Ergun, R. E., Khotyaintsev, Y., et al. (2017). Magnetospheric Multiscale mission observations of the outer electron diffusion region. *Geophysical Research Letters*, *44*, 2049–2059. https://doi.org/10.1002/2017GL072830

Hwang, K.-J., Sibeck, D. G., Giles, B. L., Pollock, C. J., Gershman, D., Avanov, L., et al. (2016). The substructure of a flux transfer event observed by the MMS spacecraft. *Geophysical Research Letters*, *43*, 9434–9443. https://doi.org/10.1002/2016GL070934

King, J. H., & Papitashvili, N. E. (2005). Solar wind spatial scales in and comparisons of hourly Wind and ACE plasma and magnetic field data. *Journal of Geophysical Research*, *110*, A02104. https://doi.org/10.1029/2004JA010649

Lee, L. C., & Fu, Z. F. (1985). A theory of magnetic flux transfer at the Earth's magnetopause. *Geophysical Research Letters*, *12*(2), 105–108. https://doi.org/10.1029/GL012i002p00105

Lindqvist, P.-A., Olsson, G., Torbert, R. B., King, B., Granoff, M., Rau, D., et al. (2016). The Spin-Plane Double Probe Electric Field Instrument for MMS. *Space Science Reviews*, *199*(1-4), 137–165. https://doi.org/10.1007/s11214-014-0116-9

Lockwood, M., Cowley, S. W. H., & Onsager, T. G. (1996). Ion acceleration at both the interior and exterior Alfvén waves associated with the magnetopause reconnection site: Signatures in cusp precipitation. *Journal of Geophysical Research*, *101*, 21,501–21,515.

Mistry, R., Eastwood, J. P., Haggerty, C. C., Shay, M. A., Phan, T. D., Hietala, H., & Cassak, P. A. (2016). Observations of Hall Reconnection Physics Far Downstream of the X Line. *Physical Review Letters*, *117*, 185102.

Mozer, F. S., Bale, S. D., & Phan, T. D. (2002). Evidence of Diffusion Regions at a Subsolar Magnetopause Crossing. *Physical Review Letters*, *89*, 015002.

Nagai, T., Shinohara, I., Fujimoto, M., Hoshino, M., Saito, Y., Machida, S., & Mukai, T. (2001). Geotail observations of the Hall current system: Evidence of magnetic reconnection in the magnetotail. *Journal of Geophysical Research*, *106*, 25929.

Nagai, T., Shinohara, I., Fujimoto, M., Machida, S., Nakamura, R., Saito, Y., & Mukai, T. (2003). Structure of the Hall current system in the vicinity of the magnetic reconnection site. *Journal of Geophysical Research*, *108*(A10), 1357. https://doi.org/10.1029/2003JA009900

Nagai, T., Shinohara, I., Fujimoto, M., Matsuoka, A., Saito, Y., & Mukai, T. (2011). Construction of magnetic reconnection in the near-Earth magnetotail with Geotail. *Journal of Geophysical Research*, *116*, A04222. https://doi.org/10.1029/2010JA016283

Nakamura, T. K. M., & Daughton, W. (2014). Turbulent plasma transport across the Earth's low-latitude boundary layer. *Geophysical Research Letters*, *41*, 8704–8712. https://doi.org/10.1002/2014GL061952

Øieroset, M., Phan, T. D., Fujimoto, M., Lin, R. P., & Lepping, R. P. (2001). In situ detection of collisionless reconnection in the Earth's magnetotail. *Nature*, *412*(6845), 414–417.

Owen, C. J., Marchaudon, A., Dunlop, M. W., Fazakerley, A. N., Bosqued, J.-M., Dewhurst, J. P., et al. (2008). Cluster observations of "crater" flux transfer events at the dayside high-latitude magnetopause. *Journal of Geophysical Research*, *113*, A07S04. https://doi.org/10.1029/2007JA012701

Paschmann, G., Baumjohann, W., Sckopke, N., Papamastorakis, I., Carlson, C. W., Sonnerup, B. U. Ö., & Lühr, H. (1986). The magnetopause for large magnetic shear—AMPTE/IRM observations. *Journal of Geophysical Research*, *91*, 11,099–11,115.

Paschmann, G., Øieroset, M., & Phan, T. (2013). In-Situ Observations of Reconnection in Space. *Space Science Reviews*, *178*, 385–417. https://doi.org/10.1007/s11214-012-9957-2

Paschmann, G., Sonnerup, B. U. Ö., Papamastorakis, I., Sckopke, N., Haerendel, G., Bame, S. J., et al. (1979). Plasma acceleration at the Earth's magnetopause: Evidence for reconnection. *Nature*, *282*, 243–246.

Phan, T. D., Eastwood, J. P., Cassak, P. A., Øieroset, M., Gosling, J. T., Gershman, D. J., et al. (2016). MMS observations of electron-scale filamentary currents in the reconnection exhaust and near the X line. *Geophysical Research Letters*, *43*, 6060–6069. https://doi.org/10.1002/2016GL069212

Phan, T. D., Paschmann, G., & Sonnerup, B. U. Ö. (1996). Low-latitude dayside magnetopause and boundary layer for high magnetic shear: 2. Occurrence of magnetic reconnection. *Journal of Geophysical Research*, *101*, 7817–7828.

Pollock, C., Moore, T., Jacques, A., Burch, J., Gliese, U., Saito, Y., et al. (2016). Fast Plasma Investigation for Magnetospheric Multiscale. *Space Science Reviews*, *199*(1-4), 331–406. https://doi.org/10.1007/s11214-016-0245-4

Pritchett, P. L. (2008). Collisionless magnetic reconnection in an asymmetric current sheet. *Journal of Geophysical Research*, *113*, A06210. https://doi.org/10.1029/2007JA012930

Retinò, A., Vaivads, A., André, M., Sahraoui, F., Khotyaintsev, Y., Pickett, J. S., et al. (2006). Structure of the separatrix region close to a magnetic reconnection X-line: Cluster observations. *Geophysical Research Letters*, *33*, L06101. https://doi.org/10.1029/2005GL024650

Rijnbeek, R. P., Cowley, S. W. H., Southwood, D. J., & Russell, C. T. (1984). A survey of dayside flux transfer events observed by ISEE-1 and ISEE-2 magnetometers. *Journal of Geophysical Research*, *89*, 786–800.

Rijnbeek, R. P., Farrugia, C. J., Southwood, D. J., Dunlop, M. W., Mier-Jedrzejowicz, W. A. C., Chaloner, C. P., et al. (1987). A magnetic boundary signature within flux transfer events. *Planetary and Space Science*, *35*, 871–878.

Robert, P., Dunlop, M. W., Roux, A., & Chanteur, G. (1998). Accuracy of current density determination. In G. Paschmann, & P. W. Daly (Eds.), *Analysis Methods for Multi-Spacecraft Data*, (pp. 395–418). Bern: International Space Science Institute.

Russell, C. T., Anderson, B. J., Baumjohann, W., Bromund, K. R., Dearborn, D., Fischer, D., et al. (2014). The Magnetospheric Multiscale Magnetometers. *Space Science Reviews*, *199*(1-4), 189–256. https://doi.org/10.1007/s11214-014-0057-3

Russell, C. T., & Elphic, R. C. (1978). Initial ISEE magnetometer results: Magnetopause observations. *Space Science Reviews*, *22*, 681–715. https://doi.org/10.1007/BF00212619

Scholer, M. (1988). Magnetic flux transfer at the magnetopause based on single X line bursty reconnection. *Geophysical Research Letters*, *15*, 291–294. https://doi.org/10.1029/GL015i004p00291

Southwood, D. J., Farrugia, C. J., & Saunders, M. A. (1988). What are flux transfer events? *Planetary and Space Science*, *36*, 503–508. https://doi.org/10.1016/0032-0633(88)90109-2

Teh, W.-L., Nakamura, T. K. M., Nakamura, R., Baumjohann, W., & Abdullah, M. (2015). On the evolution of a magnetic flux rope: Two-dimensional MHD simulation results. *Journal of Geophysical Research: Space Physics*, *120*, 8547–8558. https://doi.org/10.1002/2015JA021619

Trattner, K. J., Petrinec, S. M., Fuselier, S. A., & Phan, T. D. (2012). The location of the reconnection line: Testing the Maximum Magnetic Shear model with THEMIS observations. *Journal of Geophysical Research*, *117*, A01201. https://doi.org/10.1029/2011JA016959

Trenchi, L., Fear, R. C., Trattner, K. J., Mihaljcic, B., & Fazakerley, A. N. (2016). A sequence of flux transfer events potentially generated by different generation mechanisms. *Journal of Geophysical Research: Space Physics*, *121*, 8624–8639. https://doi.org/10.1002/2016JA022847

Trenchi, L., Marcucci, M. F., & Fear, R. C. (2015). The effect of diamagnetic drift on motion of the dayside magnetopause reconnection line. *Geophysical Research Letters*, *42*, 6129–6136. https://doi.org/10.1002/2015GL065213

Trenchi, L., Marcucci, M. F., Pallocchia, G., Consolini, G., Bavassano Cattaneo, M. B., Di Lellis, A. M., et al. (2008). Occurrence of reconnection jets at the dayside magnetopause: Double Star observations. *Journal of Geophysical Research*, *113*, A07S10. https://doi.org/10.1029/2007JA012774

Trenchi, L., Marcucci, M. F., Pallocchia, G., Consolini, G., Cattaneo, M. B., Di Lellis, A., et al. (2009). Magnetic reconnection at the dayside magnetopause with Double Star TC1 data. *Memorie della Società Astronomica Italiana*, *80*, 287.

Trenchi, L., Marcucci, M. F., Rème, H., Carr, C. M., & Cao, J. B. (2011). TC-1 observations of a flux rope: Generation by multiple X-line reconnection. *Journal of Geophysical Research*, *116*, A05202. https://doi.org/10.1029/2010JA015986

Vaivads, A., Khotyaintsev, Y., André, M., Retinò, A., Buchert, S. C., Rogers, B. N., et al. (2004). Structure of the magnetic reconnection diffusion region from four-spacecraft observations. *Physical Review Letters*, *93*, 105001.

Vaivads, A., Retinò, A., Khotyaintsev, Y. V., & André, M. (2010). The Alfvén edge in asymmetric reconnection. *Annales Geophysicae*, *28*, 1327.

Wang, R., Lu, Q., Nakamura, R., Baumjohann, W., Russell, C. T., Burch, J. L., et al. (2017). Interaction of magnetic flux ropes via magnetic reconnection observed at the magnetopause. *Journal of Geophysical Research: Space Physics*, *122*, 10,436–10,447. https://doi.org/10.1002/2017JA024482

Wang, R., Lu, Q., Huang, C., & Wang, S. (2010). Multispacecraft observation of electron pitch angle distributions in magnetotail reconnection. *Journal of Geophysical Research*, *115*, A01209. https://doi.org/10.1029/2009JA014553

Wang, R., Nakamura, R., Lu, Q., Baumjohann, W., Ergun, R. E., Burch, J. L., et al. (2017). Electron-Scale Quadrants of the Hall Magnetic Field Observed by the Magnetospheric Multiscale spacecraft during Asymmetric Reconnection. *Physical Review Letters*, *118*, 175101. https://doi.org/10.1103/PhysRevLett.118.175101

Wilder, F. D., Ergun, R. E., Goodrich, K. A., Goldman, M. V., Newman, D. L., Malaspina, D. M., et al. (2016). Observations of whistler mode waves with nonlinear parallel electric fields near the dayside magnetic reconnection separatrix by the Magnetospheric Multiscale mission. *Geophysical Research Letters*, *43*, 5909–5917. https://doi.org/10.1002/2016GL069473

Zenitani, S., Hasegawa, H., & Nagai, T. (2017). Electron dynamics surrounding the X line in asymmetric magnetic reconnection. *Journal of Geophysical Research: Space Physics*, *122*, 7396–7413. https://doi.org/10.1002/2017JA023969

Zenitani, S., & Nagai, T. (2016). Particle dynamics in the electron current layer in collisionless magnetic reconnection. *Physics of Plasmas*, *23*, 102102. https://doi.org/10.1063/1.4963008

Zenitani, S., Shinohara, I., & Nagai, T. (2012). Evidence for the dissipation region in magnetotail reconnection. *Geophysical Research Letters*, *39*, L11102. https://doi.org/10.1029/2012GL051938

Zhang, H., Kivelson, M. G., Khurana, K. K., McFadden, J., Walker, R. J., Angelopoulos, V., et al. (2010). Evidence that crater flux transfer events are initial stages of typical flux transfer events. *Journal of Geophysical Research*, *115*, A08229. https://doi.org/10.1029/2009JA015013

Zhao, C., Russell, C. T., Strangeway, R. J., Petrinec, S. M., Paterson, W. R., Zhou, M., et al. (2016). Force balance at the magnetopause determined with MMS: Application to flux transfer events. *Geophysical Research Letters*, *43*, 11,941–11,947. https://doi.org/10.1002/2016GL071568